RSC Advances

PAPER

View Article Online
View Journal | View Issue

Cite this: *RSC Adv.*, 2021, **11**, 4901

Preparation of an (inorganic/organic) hybrid hydrogel from a peptide oligomer and a tubular aluminosilicate nanofiber†

Masaru Mukai,[a] Mari Takahara,[b] Akihiko Takada[a] and Astushi Takahara *[ac]

Received 9th November 2020
Accepted 19th January 2021

DOI: 10.1039/d0ra09514a

rsc.li/rsc-advances

'Imogolite', a tubular inorganic nanotube surface, was modified with a peptide oligomer to prepare a hybrid hydrogel. The formation of the gels was confirmed by conducting a vial inversion test and rheological measurements. The surface modification of imogolite with the peptide oligomer was verified by performing thermogravimetric analysis and circular dichroism measurements. Furthermore, the formation of the network-like morphology of the prepared hydrogel was confirmed by scanning force microscopy.

Introduction

Organic–inorganic hybrid materials possess the excellent flexibility of organic materials as well as the mechanical properties of inorganic materials.[1–5] Imogolite is an aluminosilicate tubular clay material with an outer diameter of ~2.5 nm. The length of imogolite ranges from tens of nanometres to several micrometres.[6–8] Owing to its unique structure and eco-friendly nature, imogolite can be useful as an inorganic component in organic–inorganic hybrid materials.[9–11] We have previously reported the preparation and characterization of several types of imogolite-based organic–inorganic hybrid materials.[12–16] Especially, hydrogels composed of biomacromolecules–imogolite hybrid are promising for functional applications.[10,17] In practical use, the low critical gelation concentration and molecular-weight of imogolite-based hydrogel are ideal for combined biomolecules, considering the effective concentration *in vivo*.

Herein, we have focused on peptide amphiphiles (PAs) composed of hydrophilic and hydrophobic amino acids that have been widely used to prepare low-molecular-weight gelators because of their potential to control aggregation by changing the amino acid sequence.[17–23] For example, the secondary structures of PAs, such as β-sheets, contribute to the fibrous morphology of the peptide assemblies, and also act as cross-linking points for the formation of fibrous networks. In this study, we have attempted to assemble oligopeptides on the surface of imogolite to develop a hybrid hydrogel. We designed a peptide oligomer, NH_2–pSFEFE–NH_2 (isoelectric point (pI): 2.73), that possess self-assembly ability, and an anionic β-sheet-forming amino-acid sequence (FEFE)[24] as well as phosphorylated serine (pS) for imogolite absorption.[10,25–28] The C-terminal of the peptide chain was amidated to minimise electrostatic interactions.

Materials and methods

Materials

Imogolite was synthesized by previous reported methods.[29] All reagents and solvents for peptide synthesis were used without further purification. Peptides used in this study (Fig. S1†) were synthesized manually according to Fmoc-solid phase synthesis (see ESI†). The synthesized peptides were identified by mass spectrometry and NMR (Fig. S2–S6†).

Preparation of the peptide oligomer–imogolite hybrid hydrogel

The peptide oligomer (5.0 mg) was placed in a round-bottom flask, and imogolite solution (10 mL, 0.30 mg mL^{-1}, pH 9.0) was added to it. After 6 h of continuous stirring, the mixture was dialysed in a dialysis bag (6k–8k, Spectra/Por 1, Standard RC tubing) to remove excess peptide. The resulting solution (3.0 mL) was kept overnight at 4 °C in a 5 mL sample vial (inner diameter 13 mm). The gel was freeze-dried to obtain a xerogel. The weight of the xerogel was measured to determine the water content of the hybrid gel sample.

Attenuated total reflectance Fourier transform infrared (ATR-FTIR) measurements

Infrared (IR) spectra were recorded on VERTEX 70 (Bruker Co. Ltd., Massachusetts, USA) equipped with a Seagull system (Harrick Scientific Products Inc., New York, USA). All spectra

[a]*Institute for Materials Chemistry and Engineering, Kyushu University, 744 Motooka, Nishi-ku, Fukuoka 819-0395, Japan. E-mail: takahara@cstf.kyushu-u.ac.jp; Fax: +81-92-802-2516; Tel: +81-92-802-2518*

[b]*Department of Materials Science & Chemical Engineering, National Institute of Technology, Kitakyushu College, 5-20-1 Shii, Kokuraminami-ku, Kitakyushu, 802-0985, Japan*

[c]*Next Generation Adhesion Technology Research Center, Kyushu University, 744 Motooka, Nishi-ku, Fukuoka 819-0395, Japan*

† Electronic supplementary information (ESI) available: Materials, characterization, vial inversion test, TGA, XPS and NMR result. See DOI: 10.1039/d0ra09514a

were measured 128 scan between 4000 cm^{-1} and 600 cm^{-1} with a resolution of 0.5 cm^{-1} at room temperature.

Rheological measurements

Rheological measurements of peptide oligomer–imogolite hybrid (0.3 mg mL^{-1}) were carried out at 25 °C by a Physica MCR 101 rheometer (Anton Parr, Graz, Austria). Geometry of the measurements was the parallel-plate with a diameter 50 mm and a gap length 1 mm.

CD spectra measurements

CD spectra were measured with a J-720 CD spectropolarimeter (Jasco, Tokyo, Japan) using a 1 cm quartz cell at 25 °C with a scanning rate of 200 nm min^{-1} and a response time of 2 s. Concentrations of pristine imogolite and NH_2–pSFEFE–NH_2/imogolite hybrid were 0.3 mg mL^{-1} (estimated peptide concentration 7.4 μM). NH_2–pSFEFE–NH_2/imogolite hybrid hydrogel was prepared in the optical CD cell. Concentrations of free NH_2–pSFEFE–NH_2 was 0.025 mM. The CD spectra of NH_2–pSFEFE–NH_2 was measured from 190 nm to 350 nm. All spectra were background subtracted using deionized water as the blank.

Scanning force microscopy (SFM) observation

The topography of imogolite and NH_2–pSFEFE–NH_2/imogolite hybrid were visualized by scanning force microscopy (SFM, SII, SPA400). SFM samples were prepared by dip-coated on a Si wafer of 0.01 mg mL^{-1} NH_2–pSFEFE–NH_2/imogolite and pristine imogolite solutions. Persistence lengths were measured from SFM image of NH_2–pSFEFE–NH_2/imogolite and neat imogolite using ImageJ software.

Results and discussion

Preparation of the peptide oligomer–imogolite hybrid hydrogel

The chemical structure of the peptide for modification of imogolite and a schematic representation of the vial inversion test, confirming the formation of the hydrogel of the peptide oligomer–imogolite (NH_2–pSFEFE–NH_2/imogolite hybrid) hybrid, are shown in Fig. 1. The lowest gelation concentration of NH_2–pSFEFE–NH_2/imogolite hybrid was observed during the vial inversion test was 0.27 mg mL^{-1}, which is lower than the minimum gelation concentration of most PA hydrogelators (Fig. S7†).[17–23] The water content was 3700 times (by weight) the sample weight (1 g of water present in 0.27 mg of NH_2–pSFEFE–NH_2/imogolite hybrid).

Characterization of the peptide oligomer–imogolite hybrid

The adsorption of the synthesized peptide oligomer on imogolite was confirmed by attenuated total reflectance Fourier transform infrared (ATR-FTIR) spectrometry. ATR-FTIR spectra of pristine imogolite, free peptide (NH_2–pSFEFE–NH_2), NH_2–pSFEFE–NH_2/imogolite hybrid, are shown in Fig. 2. The absorption peaks at 3499, 995 and 940 cm^{-1} are ascribed to stretching vibration of O–H, Si–O and Al–O in the pristine imogolite, respectively. The absorption peaks at 3281, 2930, 1693, 1657 and 1536 cm^{-1} in ATR-FTIR spectrum of free peptide are ascribed to amide I (stretching vibration of N–H), antisymmetric vibration of CH_2, stretching vibration of aromatic ring, amide I (stretching vibration of C=O) and amide II (bending vibration of N–H), respectively. In the ATR-IR spectra of the NH_2–pSFEFE–NH_2/imogolite hybrid, both peptide-derived peaks (CH_2, aromatic ring, amide I and amide II) and imogolite-derived peaks (OH, Si–O and Al–O) were observed. This result indicated that the adsorption of NH_2–pSFEFE–NH_2 on the imogolite surface.

The physical properties of the hydrogel

The physical properties of the hydrogel were characterized on the basis of rheological measurement of the hybrid hydrogel. The storage modulus (G') and the loss modulus (G'') of the NH_2–pSFEFE–NH_2/imogolite hybrid hydrogel are shown in Fig. 3. G' was found to be greater than G'' over a wide range of angular frequencies (ω). G' was almost constant, even in the low ω

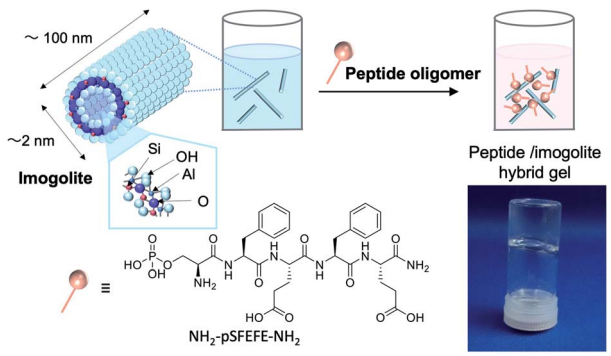

Fig. 1 Schematic diagram of hybrid gel preparation and image of the hybrid hydrogel (NH_2–pSFEFE–NH_2/imogolite hybrid (0.27 mg mL^{-1})).

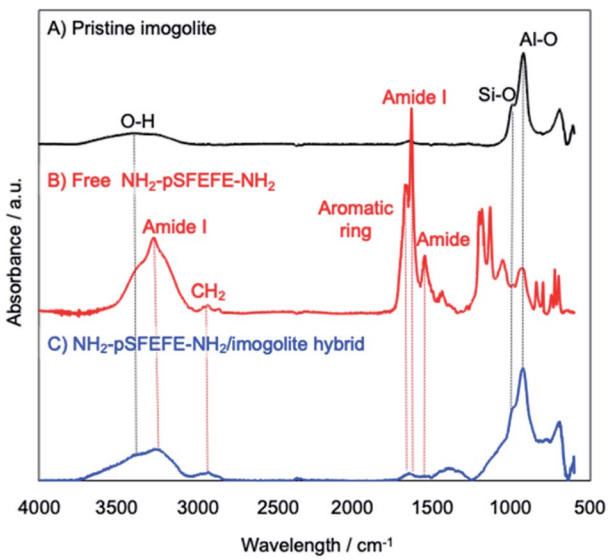

Fig. 2 ATR-FTIR spectra of (A) pristine imogolite, (B) free NH_2–pSFEFE–NH_2, (C) NH_2–pSFEFE–NH_2/imogolite hybrid.

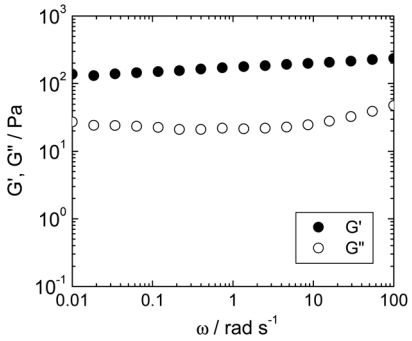

Fig. 3 Angular frequency (ω) dependence of storage modulus (G', filled circle) and loss modulus (G'', open circle) of NH_2–pSFEFE–NH_2/imogolite hybrid (0.3 mg mL^{-1}) at 25 °C.

region. These results agree with the gel characteristics and confirm that the hybrid sample behaves as a gel.

The gelation ability of the peptides with different amino acid sequences was investigated in the presence of imogolite (Fig. S1 and S8†). Gelation was not observed when the glutamic acid (E) residue in the peptide chain (peptide oligomer-modified imogolite) was replaced with cationic amino acids like lysine (K) (NH_2–pSFKFK–NH_2, pI 8.43) and arginine (R) (NH_2–pSFRFR–NH_2, pI 9.32). Partial gelation was observed in imogolites modified with peptides in which glutamic acid was replaced with aspartic acid (D) (NH_2–pSFDFD–NH_2, pI 2.57). These results suggested that anionic carboxylic acids and their alkyl chain lengths in the peptide sequences promote gelation. Gelation was not observed when the pS moiety in the peptide oligomer-modified imogolite hybrid was substituted by serine (NH_2–SFEFE–NH_2, pI 4.60). The adsorption of NH_2–pSFEFE–NH_2, NH_2–SFEFE–NH_2, NH_2–pSFKFK–NH_2, NH_2–pSFRFR–NH_2 and NH_2–pSFDFD–NH_2 on the imogolite surface were confirmed by thermogravimetric analysis (TGA) results (Table S1†). Phosphate groups are reported to have a strong tendency to be adsorbed on the imogolite surface.[10,25–28] Hence, NH_2–pSFEFE–NH_2, NH_2–pSFKFK–NH_2, NH_2–pSFRFR–NH_2 and NH_2–pSFDFD–NH_2 were adsorbed by interaction between phosphoric acid and imogolite surface. NH_2–SFEFE–NH_2 was found to be adsorbed on imogolites despite the absence of phosphate groups. The pI of imogolite has been reported to be approximately 10,[30] and the pI of NH_2–SFEFE–NH_2 was estimated to be 4.60. The peptide oligomer NH_2–SFEFE–NH_2 was non-specifically adsorbed on the imogolite surface *via* electrostatic interactions. The cationic imogolite surface effectively adsorbed carboxylic acid residues. The carboxylic acid groups present in NH_2–pSFEFE–NH_2 were considered to promote dispersibility in water by electrostatic repulsion and form a cross-linked structure by carboxylic acid dimer formation and/or dimer formation of NH_2–pSFEFE–NH_2.

The morphology of the hydrogel

Scanning force microscopy (SFM) was used to investigate the morphology of the imogolite and NH_2–pSFEFE–NH_2/imogolite hybrid (Fig. 4). Hundred-nanometre-long to several micrometre-long linear structures (typical imogolite morphology) were observed for the pristine imogolite samples. A three-dimensional fibrous network was observed for the NH_2–pSFEFE–NH_2/imogolite hybrid. The persistence lengths (L) of pristine imogolite and NH_2–pSFEFE–NH_2/imogolite hybrid were measured to be 160 ± 100 nm and 280 ± 130 nm, respectively (from the SFM images). NH_2–pSFEFE–NH_2/imogolite hybrid showed a longer persistence length (L), and a more continuous fibrous network compared to pristine imogolite. The electrostatic interactions of the pristine imogolites in neutral aqueous solutions hindered the formation of network-like structures.[14,29] The heights of pristine imogolite (H) and NH_2–pSFEFE–NH_2/imogolite hybrid were measured using the SFM images, and were found to be 2.4 ± 0.3 nm and 4.2 ± 0.6 nm, respectively. As the expanded molecular length of NH_2–pSFEFE–NH_2 was 2.1 nm, it was determined that NH_2–pSFEFE–NH_2 has a tilted geometry and is absorbed on the surface of imogolite. In NH_2–pSFEFE–NH_2/imogolite hybrid, non-covalent bonding such as hydrogen bonding, π–π stacking, CH–π interactions, and non-polar interactions were expected because peptide oligomers are present. A continuous fibrous network was formed due to the cross-linking structure between the imogolites. The aspect ratio of NH_2–pSFEFE–NH_2/imogolite hybrid is defined as the divided height ($H = 4.2 \pm 0.6$ nm) by persistence length ($L = 280 \pm 130$ nm), and it has a high aspect ratio of 67. The high aspect ratio of NH_2–pSFEFE–NH_2/imogolite hybrid might contribute to low percolation threshold indicated by a low minimum gelation concentration of NH_2–pSFEFE–NH_2/imogolite hybrid.

CD spectra measurements of the peptide oligomer on imogolite

Fig. 5 shows the circular dichroism (CD) spectra of free NH_2–pSFEFE–NH_2, pristine imogolite, and NH_2–pSFEFE–NH_2/

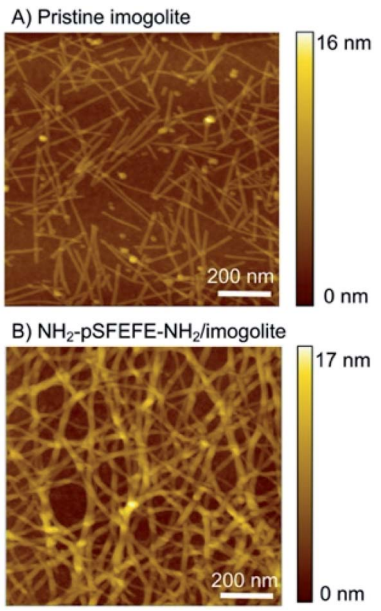

Fig. 4 SFM image of (A) pristine imogolite and (B) NH_2–pSFEFE–NH_2/imogolite hybrid on Si wafer substrate.

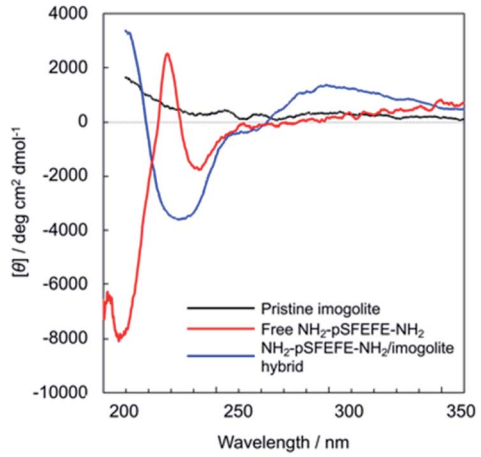

Fig. 5 CD spectra of free NH_2–pSFEFE–NH_2 (red line), pristine imogolite (black line), and NH_2–pSFEFE–NH_2/imogolite hybrid (blue line).

imogolite hybrid. The spectrum of the pristine imogolite solution was CD silent in this wavelength range. A minimum at 197 nm and a positive band around 220 nm in the CD spectral profile of free NH_2–pSFEFE–NH_2 indicated a random coil structure. A positive band around 200 nm and a negative broad peak around 220 nm in NH_2–pSFEFE–NH_2/imogolite hybrid were ascribed to π–π* or n–π* transition of CO–NH, respectively, which is characteristic for the formation of β-sheet structure in the peptide. Changes in CD spectra after addition of imogolite to NH_2–pSFEFE–NH_2 solution indicated that the peptide interacts with imogolite forming β-sheet formation. Therefore, β-sheet structure of the peptide was supposed to induce its adsorption on imogolite in addition to electrostatic interaction by pS moiety and FEFE sequence. Also, the secondary structure content was estimated from the CD spectra of free NH_2–pSFEFE–NH_2 and NH_2–pSFEFE–NH_2/imogolite hybrid using the BeStSel programme (Table S1†).[31,32] After imogolite addition, the percentage of the parallel β-sheet in NH_2–pSFEFE–NH_2 significantly increased from 0% to 22.1%, and the percentage of the anti-parallel β-sheet decreased from 26.0% to 1.8%. These results suggested that the phosphate groups in the peptide chain might dictate its orientation on imogolite, resulting in the parallel β-sheet formation of NH_2–pSFEFE–NH_2 whose orientation toward imogolite is homogeneous. X-ray photoelectron spectroscopy (XPS), and TGA were used to confirm the adsorption of NH_2–pSFEFE–NH_2 on the imogolite surface (Table S2 and Fig. S9†). The TGA results revealed that glutamic acid and pS residues contributed to the increased peptide adsorption on the imogolite surface. The peptide containing the pS moiety and FEFE amino-acid sequence specifically facilitated the peptide adsorption on the imogolite surface because of anionic and β-sheet forming nature of pSFEFE. This result is consistent with the gelation ability toward imogolite, as previously described. Thus, it is reported that a simple peptide gelator for an imogolite substrate *via* adsorption is promising for inorganic–organic material platforms.

Conclusions

We prepared a peptide oligomer-modified imogolite substrate. The excellent hydrogelation ability of the hybrid material was confirmed by vial inversion and rheological tests. SFM observations confirmed the three-dimensional network of hydrogels formed by the peptide oligomer-modified imogolite. Changes in the gelation ability of the peptide sequences suggested that phosphate and carboxylic acid groups contribute to the gelation ability. CD spectra suggested that peptide oligomer accumulation on the surface of the imogolite contributed to the gelation by its β-sheet formation. Thus, this is a simple and applicable method for preparing self-assembled inorganic–organic hybrid materials. The peptides/imogolite hybrid hydrogel is a promising biomaterial for applications such as cell culture scaffolds. Imogolite has been reported to be an effective scaffold for cells[33] due to its biocompatible and flexible design. Hence, the imogolite-based gels can be potentially used in various fields.

Conflicts of interest

There are no conflicts to declare.

Acknowledgements

The authors acknowledge the financial support of JSPS Grant-in-Aid for Scientific Research (Grant No. 26248053, 17H01221 to A. T. and No. 19K15369 to M. T.) and JSPS A3 Project.

References

1 J. Zhu, T. Wang, R. Zhu, F. Ge, J. Wei, P. Yuan and H. He, *Appl. Clay Sci.*, 2011, **51**, 317–322.
2 G. Lazzara, G. Cavallaro, A. Panchal, R. Fakhrullin, A. Stavitskaya, V. Vinokurov and Y. Lvov, *Curr. Opin. Colloid Interface Sci.*, 2018, **35**, 42–50.
3 Y. Lvov, K. Ariga, I. Ichinose and T. Kunitake, *J. Am. Chem. Soc.*, 1995, **117**, 6117–6123.
4 F. Geng, R. Ma, A. Nakamura, K. Akatsuka, Y. Ebina, Y. Yamauchi, N. Miyamoto, Y. Tateyama and T. Sasaki, *Nat. Commun.*, 2013, **4**, 1632.
5 P. Luo, Y. Zhao, B. Zhang, J. Liu, Y. Yang and J. Liu, *Water Res.*, 2010, **44**, 1489–1497.
6 O. Arnalds, in *Advances in Agronomy*, ed. D. L. Sparks, Academic Press, 2013, vol. 121, pp. 331–380.
7 P. D. G. Cradwick, V. C. Farmer, J. D. Russell, C. R. Masson, K. Wada and N. Yoshinaga, *Nat. Phys. Sci.*, 1972, **240**, 187–189.
8 K. Wada and N. Yoshinaga, *Am. Mineral.*, 1969, **54**, 50–71.
9 Y. Arai, M. McBeath, J. R. Bargar, J. Joye and J. A. Davis, *Geochim. Cosmochim. Acta*, 2006, **70**, 2492–2509.
10 N. Inoue, H. Otsuka, S.-I. Wada and A. Takahara, *Chem. Lett.*, 2006, **35**, 194–195.
11 W. C. Ackerman, D. M. Smith, J. C. Huling, Y. W. Kim, J. K. Bailey and C. J. Brinker, *Langmuir*, 1993, **9**, 1051–1057.
12 K. Yamamoto, H. Otsuka, S.-I. Wada, D. Sohn and A. Takahara, *Soft Matter*, 2005, **1**, 372–377.

13 K. Yamamoto, H. Otsuka, A. Takahara and S.-I. Wada, *J. Adhes.*, 2002, **78**, 591–602.
14 A. Takahara and Y. Higaki, in *Functional Polymer Composites with Nanoclays*, The Royal Society of Chemistry, 2017, pp. 131–156.
15 L. Li, A. Takada, W. Ma, S. Fujikawa, M. Ariyoshi, K. Igata, M. Okajima, T. Kaneko and A. Takahara, *Langmuir*, 2020, **36**, 1718–1726.
16 L. Li, W. Ma, A. Takada, N. Takayama and A. Takahara, *Biomacromolecules*, 2019, **20**, 3566–3574.
17 N. Javid, S. Roy, M. Zelzer, Z. Yang, J. Sefcik and R. V. Ulijn, *Biomacromolecules*, 2013, **14**, 4368–4376.
18 D. Koda, T. Maruyama, N. Minakuchi, K. Nakashima and M. Goto, *Chem. Commun.*, 2010, **46**, 979–981.
19 M. Mukai, H. Minamikawa, M. Aoyagi, M. Asakawa, T. Shimizu and M. Kogiso, *Soft Matter*, 2012, **8**, 11979–11981.
20 M. Mukai, H. Minamikawa, M. Aoyagi, M. Asakawa, T. Shimizu and M. Kogiso, *J. Colloid Interface Sci.*, 2013, **395**, 154–160.
21 K. Hanabusa, R. Tanaka, M. Suzuki, M. Kimura and H. Shirai, *Adv. Mater.*, 1997, **9**, 1095–1097.
22 C. Tomasini and N. Castellucci, *Chem. Soc. Rev.*, 2013, **42**, 156–172.
23 S. Kiyonaka, K. Sada, I. Yoshimura, S. Shinkai, N. Kato and I. Hamachi, *Nat. Mater.*, 2004, **3**, 58–64.
24 R. J. Swanekamp, J. T. M. DiMaio, C. J. Bowerman and B. L. Nilsson, *J. Am. Chem. Soc.*, 2012, **134**, 5556–5559.
25 N. Jiravanichanun, K. Yamamoto, K. Kato, J. Kim, S. Horiuchi, W.-O. Yah, H. Otsuka and A. Takahara, *Biomacromolecules*, 2012, **13**, 276–281.
26 W. Ma, H. Otsuka and A. Takahara, *Chem. Commun.*, 2011, **47**, 5813–5815.
27 W. O. Yah, A. Irie, H. Otsuka, S. Sasaki, N. Yagi, M. Sato, T. Koganezawa and A. Takahara, *J. Phys.: Conf. Ser.*, 2011, **272**, 012021.
28 W. Ma, J. Kim, H. Otsuka and A. Takahara, *Chem. Lett.*, 2011, **40**, 159–161.
29 V. C. Farmer, A. R. Fraser and J. M. Tait, *J. Chem. Soc., Chem. Commun.*, 1977, 462–463.
30 N. Arancibia-Miranda, M. Escudey, M. Molina and M. T. García-González, *J. Non-Cryst. Solids*, 2011, **357**, 1750–1756.
31 A. Micsonai, F. Wien, L. Kernya, Y.-H. Lee, Y. Goto, M. Réfrégiers and J. Kardos, *Proc. Natl. Acad. Sci. U. S. A.*, 2015, **112**, E3095.
32 A. Micsonai, F. Wien, É. Bulyáki, J. Kun, É. Moussong, Y. H. Lee, Y. Goto, M. Réfrégiers and J. Kardos, *Nucleic Acids Res.*, 2018, **46**, W315–W322.
33 K. Ishikawa, T. Akasaka, Y. Nodasaka, N. Ushijima, M. Kaga, S. Abe, M. Uo, Y. Yawaka, M. Suzuki and F. Watari, *Nano Biomedicine*, 2009, **1**, 109–120.